Xiang Chen
The State Key Laboratory of Tribology and
Institute of Manufacturing Engineering,
Department of Mechanical Engineering,
Tsinghua University,
Beijing 100084, China

Chao Chen[1]
Mem. ASME
Department of Mechanical
and Aerospace Engineering,
Monash University,
Clayton, Victoria 3802, Australia
e-mail: chao.chen@monash.edu

Xin-Jun Liu[1]
The State Key Laboratory of Tribology and
Institute of Manufacturing Engineering,
Department of Mechanical Engineering,
Tsinghua University,
Beijing 100084, China
e-mail: xinjunliu@mail.tsinghua.edu.cn

Evaluation of Force/Torque Transmission Quality for Parallel Manipulators

Performance evaluation is one of the most important issues in the analysis and design of parallel manipulators. The internal forces and torques in parallel manipulators contribute to manipulating the end-effectors and resisting the external loads. In this work, we propose a transmission index to evaluate the force and torque transmission quality of parallel manipulators. The index is normalized and used to analyze the exactly constrained parallel manipulators, based on the transmission matrix spanned by transmission wrench screws (TWSs). Furthermore, the index is applied to parallel manipulators with different degrees of freedom (DOF) in order to illustrate and validate the proposed approach and index. Finally, a typical parallel manipulator is selected to address the comparison analysis between different indices, which demonstrates that the proposed index, possessing respective merits, could be complementary to other existing indices.
[DOI: 10.1115/1.4029188]

Keywords: transmission index, transmission wrench screw, parallel manipulator

1 Introduction

Parallel manipulators are, nowadays, leaving academic laboratories and finding their ways in an increasing number of application fields, such as machine tool, fast manipulating, and flight simulator [1]. Performance analysis of parallel manipulators is one of the most significant and challenging problems. Especially in the analysis of parallel manipulators with specific motions, the force transmissibility evaluation is significant and remains to be solved.

When a parallel manipulator executes a given task, such as grinding, grasping, brushing, and lifting up, it balances the contact forces and torques on its end-effector from joint space by the joint force/torque. Therefore, the internal transmission forces in a parallel manipulator play key roles in manipulating the end-effector and resisting external loads. Actually, the transmission quality of the output force/torque is studied in this paper.

In the last few decades, much effort has been devoted toward the force transmission performance analysis of parallel manipulators, and several approaches are now at hand. The approaches can mainly be categorized into three items: force Jacobian matrix method, manipulability analysis method, and static performance analysis method. Force Jacobian matrix, a map of the force and torque from the joint space to the task space, was primarily used in the force transmission analysis of mechanisms [2–4]. The condition number of the force Jacobian matrix was used to evaluate the force transmissibility [5]. The concept of manipulability, in terms of the ability to move and apply forces in arbitrary directions, was first proposed by Salisbury and Craig [6], while Yoshikawa [7] introduced a comprehensive manipulability ellipsoids approach to measure the force transmissibility (manipulability) of serial manipulators. Static performance analysis concerns about the relationship of forces and motions between inputs and output of a manipulator. This approach can be divided into two aspects, i.e., forward and inverse force transmission analysis. The former one attempts to find the extreme magnitudes and directions of the force/torque vectors of the end-effector, when the forces of the actuators are known [8,9]. Merlet [10] proposed an efficient estimation of the external forces of a parallel manipulator in the translational workspace. Conversely, the inverse force transmission analysis is to determine the magnitude bounds of actuators for given magnitudes of the external forces and torques [11]. This method is always used for actuator size design of parallel manipulators. Both aspects consider the force relationships between joint and task forces directly, but not manifest the essential transmission property of the parallel manipulators. Basically, the larger of the actuator size, the larger external forces and torques the mechanism could bear no matter with the essential transmission performance at different configurations. A new approach which is different from any of the mentioned methods is proposed here: evaluation of the magnitude of force/torque of *transmission wrench* based on given loads on the end-effector. Based on the approach, we propose a new index which is rooted on pressure angle or transmission angle in the single DOF manipulator.

Another issue about the force/torque transmission performance analysis is the well-known unit inhomogeneous problem [12]. When we consider a mixed-DOF parallel manipulator (those with translations and rotations together), an intuitive question arises: how can we consider the force and torque together with different units? This is a widely discussed question when using the conventional Jacobian matrix. Kosuge et al. [13] separately considered the translationability and rotationability of a manipulator based on the pure forces and pure torques, respectively. However, neither of the kinematic ability could completely represent the performance of a parallel manipulator with mixed DOFs. In this work, this problem is tackled by scaling a parallel manipulator to a size with a unit characteristic length and applies a unit wrench on the platform, which will be discussed in Sec. 2.

The reminder of this work is organized as follows. Section 2 introduces the new index with its derivation for force/torque transmission performance analysis. In Sec. 3, the index is applied to a series of parallel manipulators with different DOFs to illustrate the application and validate the physical meanings. Comparison study between the proposed and existing indices are given in Sec. 4. Finally, Sec. 5 concludes this work.

[1]Corresponding author.

Manuscript received April 26, 2014; final manuscript received November 13, 2014; published online April 6, 2015. Assoc. Editor: Yuefa Fang.

2 Definition of Force/Torque Transmission Index

A parallel manipulator must transmit the joint forces and torques to the output platform, resisting the external loads, through its mechanical structure. In the process of force transmission, the arising internal wrenches, namely, the transmission wrenches, can be expressed by the TWS. It is known that a TWS must be reciprocal to the twist screws permitted by the passive joints in the corresponding leg, when the active joints are locked [14]. It should be noted that, in this study, all the considered parallel manipulators are exactly constrained systems, rather than overconstrained ones.

As shown in Fig. 1, a platform is exactly constrained by a set of TWSs, $\boldsymbol{w}_i (i = 1, 2, ..., n)$. Notably, the number of TWSs, n, varies for different cases, such as for a spatial six-dimensional case, $n = 6$, for a three-dimensional case, $n = 3$, and $n = 2$ for a two-dimensional case, which can be represented as

$$\boldsymbol{w}_i = f_i \begin{bmatrix} \boldsymbol{e}_i \\ \boldsymbol{c}_i \times \boldsymbol{e}_i + h_i \boldsymbol{e}_i \end{bmatrix} \quad i = 1, 2, ..., n \tag{1}$$

where $\boldsymbol{e}_i$ is the unit directional vector of the TWS, $\boldsymbol{c}_i$ is the vector pointing from the center of the platform to the characteristic point of the ith leg, which is defined as the physical center of the last passive joint in the leg, h_i is the pitch of the TWS, and f_i is the magnitude of the TWS in terms of force. For a pure force, the pitch of the wrench is zero. The unit characteristic length is then defined as the distance from the center of the platform to the farthest characteristic point of the passive joint attached to the platform. Further, the parallel manipulator under study is always scaled to a size with the unit characteristic length for a consistent evaluation. For a pure torque, the TWS with infinite pitch can be written as $\tau \begin{bmatrix} \boldsymbol{0}^{\mathrm{T}} & \boldsymbol{e}^{\mathrm{T}} \end{bmatrix}^{\mathrm{T}}$, where τ is the magnitude of the TWS in terms of torque.

Given a load wrench, $\boldsymbol{W}$, on the platform, we must have

$$\boldsymbol{W} = \sum_{i=1}^{n} \boldsymbol{w}_i \tag{2}$$

To consistently evaluate the performance of the system in resisting the load, we apply a unit load wrench ($\|\boldsymbol{W}\| = 1$) on the platform. The unit wrench, as shown in Fig. 2, can be written as

$$\boldsymbol{W} = \begin{bmatrix} \boldsymbol{m} \\ \boldsymbol{n} \end{bmatrix} = f \begin{bmatrix} \boldsymbol{e} \\ (\boldsymbol{c} \times \boldsymbol{e}) + h\boldsymbol{e} \end{bmatrix} = f \begin{bmatrix} \boldsymbol{e} \\ (\boldsymbol{c} \times \boldsymbol{e}) \end{bmatrix} + \tau \begin{bmatrix} 0 \\ \boldsymbol{e} \end{bmatrix} \tag{3}$$

where h is the pitch, the torque magnitude is given by $\tau = fh$, and $\boldsymbol{c}$ is the vector pointing at the action point of the wrench, which is constrained on a unit sphere. Without loss of generality, the force magnitude f is assumed to nonnegative. Since $f = \|\boldsymbol{m}\|$ and $\|\boldsymbol{m}\|^2 + \|\boldsymbol{n}\|^2 = 1$, the force magnitude is not greater than 1. It is not difficult to see that the torque magnitude is between -1 and $+1$ due to the unit vector $\|\boldsymbol{W}\|$.

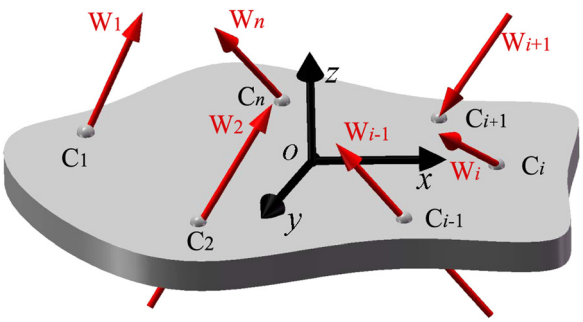

Fig. 1 A platform constrained by a set of TWSs

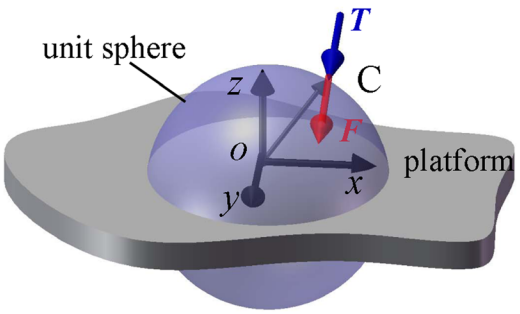

Fig. 2 Unit wrench on the platform

In the case of pure force acting on the center of the platform, the moment must be zero and $f = 1$. Hence, the wrench can be written as $\boldsymbol{W} = \begin{bmatrix} \boldsymbol{e}^{\mathrm{T}} & \boldsymbol{0}^{\mathrm{T}} \end{bmatrix}^{\mathrm{T}}$. In the case of pure moment, f must be zero and h is infinity. Hence, we have $\boldsymbol{W} = \begin{bmatrix} \boldsymbol{0}^{\mathrm{T}} & \boldsymbol{e}^{\mathrm{T}} \end{bmatrix}^{\mathrm{T}}$ with unit torque magnitude. A general unit wrench, as shown in Fig. 2, is the combination of force and torque acting on the point constrained on a unit sphere centered at the center of the platform. Further, this unit sphere must contain the characteristic point with a distance of the unit characteristic length from the center.

When a unit wrench is applied, the transmission wrenches are consequently generated. The magnitudes of the transmission wrenches indicate the performance of the system, i.e., the less the magnitudes of the wrenches are, the better the system is capable of transmitting the forces and torques to the platform, and vice versa. This idea is fundamentally equivalent to the meanings of the pressure angle and transmission angle [15]. The main difference is that the pressure and transmission angles are usually used to deal with 1DOF system, where the load can represented by a scalar. Here, the Euclidean norm of the magnitudes of TWSs is used for evaluation.

Substituting Eq. (1) into Eq. (2) yields

$$\boldsymbol{E}\boldsymbol{F} = \boldsymbol{W} \tag{4}$$

where $\boldsymbol{W}$ is the unit wrench, $\boldsymbol{F} = \begin{bmatrix} f_1 & f_2 & \dots & f_n \end{bmatrix}^{\mathrm{T}}$, and $\boldsymbol{E}$ is termed transmission matrix [16,17]

$$\boldsymbol{E} = \begin{bmatrix} \boldsymbol{e}_1 & \boldsymbol{e}_2 & \dots & \boldsymbol{e}_n \\ (\boldsymbol{c}_1 \times \boldsymbol{e}_1) + h_1 \boldsymbol{e}_1 & (\boldsymbol{c}_2 \times \boldsymbol{e}_2) + h_2 \boldsymbol{e}_2 & \dots & (\boldsymbol{c}_n \times \boldsymbol{e}_n) + h_n \boldsymbol{e}_n \end{bmatrix} \tag{5}$$

The singular values of $\boldsymbol{E}$ are the semi-axes of the n-dimensional ellipsoid to which a unit n-dimensional sphere is mapped by $\boldsymbol{E}$. Therefore, these singular values represent the extreme cases when the unit wrench is collinear with left-singular vectors. For singular value σ_i of $\boldsymbol{E}$, we have

$$\boldsymbol{E}\boldsymbol{v}_i = \sigma_i \boldsymbol{u}_i \tag{6}$$

where $\boldsymbol{u}_i$ and $\boldsymbol{v}_i$ are the left- and right-singular vectors, respectively, of σ_i. Equation (6) can be rewritten as

$$\boldsymbol{E}\boldsymbol{v}_i/\sigma_i = \boldsymbol{u}_i = \boldsymbol{W} \tag{7}$$

Comparing Eqs. (4) and (7), we could yield the solution $\boldsymbol{F}_i = \boldsymbol{v}_i/\sigma_i$ by considering $\boldsymbol{W} = \boldsymbol{u}_i$. Since singular vectors are unit vectors we must have $\|\boldsymbol{F}_i\|^2 = 1/\sigma_i^2$. By considering all the extreme cases indicated by the semi-axes, an indicator of the performance can be defined as the sum of the norms of $\boldsymbol{F}_i$, i.e.,

$$\mathrm{PI} = \sum \|\boldsymbol{F}_i\|^2 = \sum 1/\sigma_i^2 \tag{8}$$

The less PI is, the better the output force/torque transmission performance is the system. However, PI may have a value of infinity when parallel singularity (the worst scenario) is encountered. The normalized performance index (NPI) is then defined as

$$\text{NPI} = \text{PI}_{\min}/\text{PI} \tag{9}$$

where $\text{PI}_{\min}$ is the possible minimum value PI can reach in the system.

THEOREM 1. *PI_{min} with respect to $\boldsymbol{E}$ given by Eq. (5) for a n-dimensional ($n=3,6$) parallel manipulator is $n^2/(2n+\sum h_i^2)$.*

Proof. According to Eq. (5), the trace of $\boldsymbol{E}^{\mathrm{T}}\boldsymbol{E}$ is given by

$$\text{trace} = n + \sum \|\boldsymbol{c}_i \times \boldsymbol{e}_i\|^2 + \sum h_i^2 \quad i = 1, 2, ..., n \tag{10}$$

where $n = 3$ for three-dimensional planar parallel manipulator, while $n = 6$ for six-dimensional spatial parallel manipulator.

Since the characteristic length being the maximum norm of c_i is one, $\|c_i \times \boldsymbol{e}_i\|$ is no greater than one. Hence, we have

$$\sum \sigma_i^2 = \text{trace} \le 2n + \sum h_i^2 = k \tag{11}$$

To find the minimum of PI, the object function with Lagrange multiplier is defined as

$$\text{obj} = \sum 1/\sigma_i^2 + \lambda(k - \sum \sigma_i^2 - s^2) \tag{12}$$

where s is a slack variable converting the inequality (11) to an equality constraint.

The zero conditions of partial differentiation with respect to σ_i^2 and s yields $s = 0$ and

$$\sigma_i = k/n \tag{13}$$

Hence,

$$\text{PI}_{\min} = n^2/k = n^2/\left(2n + \sum h_i^2\right) \tag{14}$$

Proof completed.

Particularly in the two-dimensional case, the end-effector of this parallel manipulator always degenerates into a point rather than a platform. And the TWSs should always act on the end-effector (the point), that is to say, the characteristic length is zero, $\boldsymbol{c}_i = 0 (i = 1, 2)$. Thus, Corollary 1 is given for two-dimensional case.

COROLLARY 1. *PI_{min} with respect to $\boldsymbol{E}$ given by Eq. (5) for a two-dimensional planar parallel manipulator is $4/(2+\sum h_i^2)$.*

Proof. According to Eq. (5), the trace of $\boldsymbol{E}^{\mathrm{T}}\boldsymbol{E}$ is given by

$$\text{trace} = 2 + \sum \|\boldsymbol{c}_i \times \boldsymbol{e}_i\|^2 + \sum h_i^2 \quad i = 1, 2, 3 \tag{15}$$

Since $\|\boldsymbol{c}_i \times \boldsymbol{e}_i\|$ is always zero, we have

$$\sum \sigma_i^2 = \text{trace} \le 2 + \sum h_i^2 = k \tag{16}$$

Similar with the analysis method of the three- and six-dimensional cases, the object function with Lagrange multiplier is defined as

$$\text{obj} = \sum 1/\sigma_i^2 + \lambda(k - \sum \sigma_i^2 - s^2) \tag{17}$$

The zero conditions of partial differentiation with respect to σ_i^2 and s yields $s = 0$ and

$$\sigma_i = k/2 \tag{18}$$

Hence,

$$\text{PI}_{\min} = 4/k = 4/(2 + \sum h_i^2) \tag{19}$$

Proof completed.

Therefore, recalling to Eq. (9), the NPI can be concluded for two-, three-, and six-dimensional cases as Eqs. (20), (21), and (22), respectively.

$$\text{NPI} = \frac{4}{\left(2 + \sum h_i^2\right) \sum 1/\sigma_i^2} \quad i = 1, 2 \tag{20}$$

$$\text{NPI} = \frac{9}{\left(6 + \sum h_i^2\right) \sum 1/\sigma_i^2} \quad i = 1, 2, 3 \tag{21}$$

$$\text{NPI} = \frac{36}{\left(12 + \sum h_i^2\right) \sum 1/\sigma_i^2} \quad i = 1, 2, ..., 6 \tag{22}$$

3 Examples

Some typical parallel manipulators, including two-dimensional cases (planar parallel manipulators with two translations), three-dimensional cases (planar parallel manipulators with two translations and one rotation), and six-dimensional cases (spatial parallel manipulators), are taken as examples to illustrate the application of the proposed approach and index.

3.1 Two-Dimensional Planar Parallel Manipulators

Example 1: RPRPR Parallel Manipulator. Figure 3 shows the sketch of a RPRPR planar parallel manipulator, which has two translational DOFs. The two prismatic joints are actuated.

As an initial step, we should analyze the TWS in each leg of the RPRPR parallel manipulator. In the RPR leg, i.e., leg AC, we can achieve three twists: two passive twists, $\$_1$ and $\$_3$, corresponding to two revolute joints, and one actuated twist, $\$_2$, regarding to the prismatic joint. Since the output twist screw is limited in two-dimensional plane, the TWS degenerated into the form of $\boldsymbol{e} = (e_x, e_y, 0)$. Using reciprocal product, we can calculate the TWS in each leg, which is reciprocal to both the passive twists except the actuated twist

$$\boldsymbol{e}_1 \circ \$_i = 0 \quad (i = 1, 3) \tag{23}$$

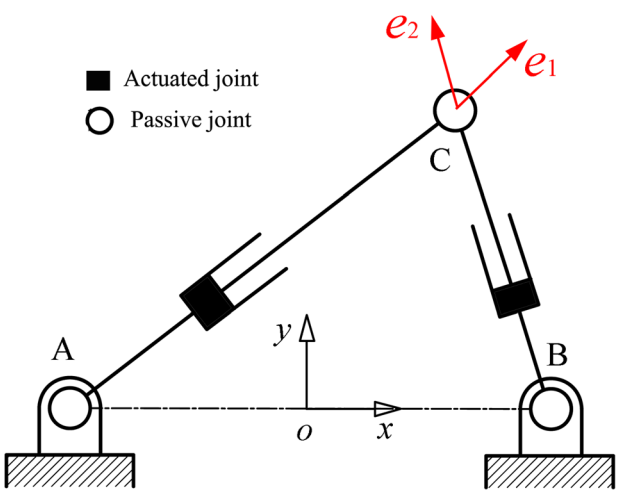

Fig. 3 A RPRPR parallel manipulator

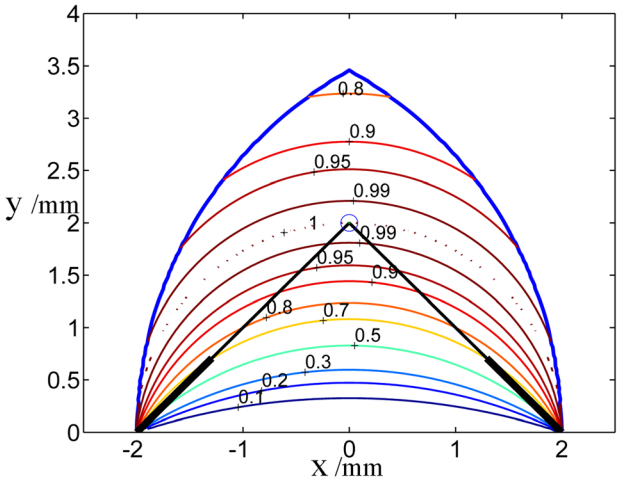

Fig. 4 Distribution of the NPI in the workspace of RPRPR parallel manipulator

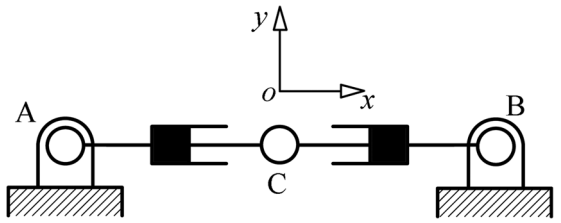

Fig. 5 A parallel singular configuration of RPRPR parallel manipulator

As shown in Fig. 3, the TWSs $\boldsymbol{e}_i (i = 1, 2)$ in both legs, with zero pitches $h_i = 0 (i = 1, 2)$, are pure forces passing through each revolute joint (joint A or B) and the end-effector (joint C). The vectors pointing at the action point of the wrench are zero, $\|\boldsymbol{c}_i\| = 0 (i = 1, 2)$. Thus, we can yield the transmission matrix as $\boldsymbol{E} = \begin{bmatrix} \boldsymbol{e}_1^{\mathrm{T}} & \boldsymbol{e}_2^{\mathrm{T}} \end{bmatrix} = \begin{bmatrix} \boldsymbol{e}_{1x} & \boldsymbol{e}_{2x} \\ \boldsymbol{e}_{1y} & \boldsymbol{e}_{2y} \\ 0 & 0 \end{bmatrix}$.

According to the defined force/torque transmission index, Eq. (20), we can write the index for this RPRPR mechanism as

$$\mathrm{NPI} = \frac{2}{1/\sigma_1^2 + 1/\sigma_2^2} \tag{24}$$

where $\sigma_i (i = 1, 2)$ is the singular value of matrix $\boldsymbol{E}$.

Without loss of generality, we assume the parameters of the manipulator as $l_{Ao} = l_{Bo} = 2$. Figure 4 illustrates the distribution of the output force/torque transmission index within the translational workspace of RPRPR parallel manipulator. The outer blue lines indicate the chosen workspace boundary with the limitation of what the extensible legs could extend. From the index distribution atlas, we can conclude that the larger NPI index it is, the better output force/torque transmissibility the mechanism performs. As shown in Fig. 4, the mechanism performs the best when the two limbs are perpendicular to each other. On the other hand, the manipulator is indicated to perform the worst force/torque transmissibility when the two limbs are collinear, yielding a parallel singularity as shown in Fig. 5.

3.2 Three-Dimensional Planar Parallel Manipulators

Example 2: 3-RRR Parallel Manipulator. Figure 6 shows a 3-RRR manipulator, a typical planar parallel mechanism, which has three identical RRR limbs connected to the base and moving

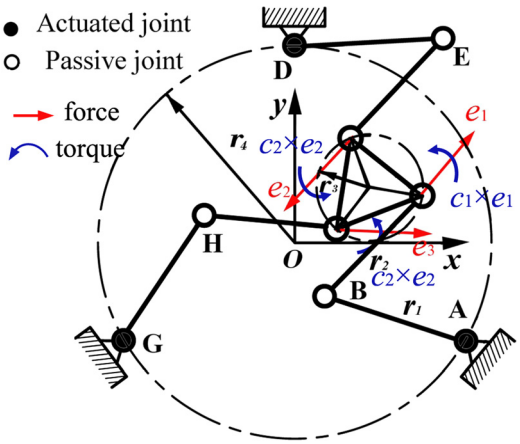

Fig. 6 A 3-RRR manipulator

platform. Due to the assumption of the unit characteristic length, we set the radius of moving platform being unity, $r_3 = 1$, hence the vectors from center of platform to the transmission force are unit vectors, $\|\boldsymbol{c}_i\| = 1 (i = 1, 2, 3)$. And other parameters of the 3-RRR manipulator are assumed as follows: the radius of the base, $r_4 = 10$, and the lengths of limbs, $r_1 = r_2 = 7$.

As analyzed in the RPRPR manipulator, the transmission force in each RRR leg is a pure force passing through two passive joints (Fig. 6), denoted as $\boldsymbol{e}_i = (e_{ix}, e_{iy}, 0), (i = 1, 2, 3)$. The distinction of the TWSs between the 3-RRR and RPRPR parallel manipulators is that the unit vectors pointing at the action point of the transmission force are $\boldsymbol{c}_i = (c_{ix}, c_{iy}, 0)$ in 3-RRR manipulator, while being zero, $\boldsymbol{c}_i = (0, 0, 0)$ in RPRPR manipulator. Hence, from Eq. (5), we can achieve the transmission matrix as $\boldsymbol{E} = \begin{bmatrix} e_{1x} & e_{2x} & e_{3x} \\ e_{1y} & e_{2y} & e_{3y} \\ e_{1x}c_{1y} - e_{1y}c_{1x} & e_{2x}c_{2y} - e_{2y}c_{2x} & e_{3x}c_{3y} - e_{3y}c_{3x} \end{bmatrix}$ which is simplified into a 3×3 matrix in this three-dimensional case.

Then, according to Eq. (21), we define the index for the 3-RRR parallel manipulator as

$$\mathrm{NPI} = \frac{3}{2(1/\sigma_1^2 + 1/\sigma_2^2 + 1/\sigma_3^2)} \tag{25}$$

where $\sigma_i (i = 1, 2, 3)$ is the singular value of the transmission matrix $\boldsymbol{E}$.

As mentioned, the 3-RRR parallel manipulator has two translational DOFs and one rotational DOF. It is hard to present the distribution of the index varied in both translational and rotational workspaces in one Figure. Thus, we draw the distribution of index in the translational workspace with some distinct rotational angles. For example, Fig. 7 shows the distribution of the index with zero constant rotational angle, and Fig. 8 is the distribution with rotational angle, $\varphi = -30$ deg, in which there exist some points with zero index values, i.e., NPI = 0.

All the outer blue lines in Figs. 7 and 8 indicate the workspace boundary corresponding to serial singular configurations. From both figures, we can draw the conclusion that the 3-RRR manipulator performs better when it is closer to the central point of the workspace. On the other hand, the translational workspace of the manipulator varies with the change of the rotational angles, and the output force/torque transmission performance differs as well. Especially, when the rotational angle is equal to -30 deg, the index value is much smaller, and there even exist some points with zero index values. The smaller index values indicate poorer force transmission performance.

Besides, we draw a figure indicating the relationship between the NPI index and rotational angles with constant position coordinates, i.e., $x = 0, y = 0$ (Fig. 9).

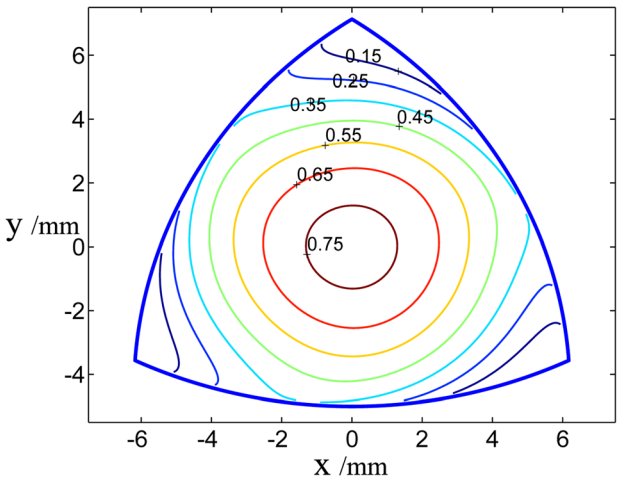

Fig. 7 Distribution of the index in the translational workspace with rotational angle $\varphi = 0$

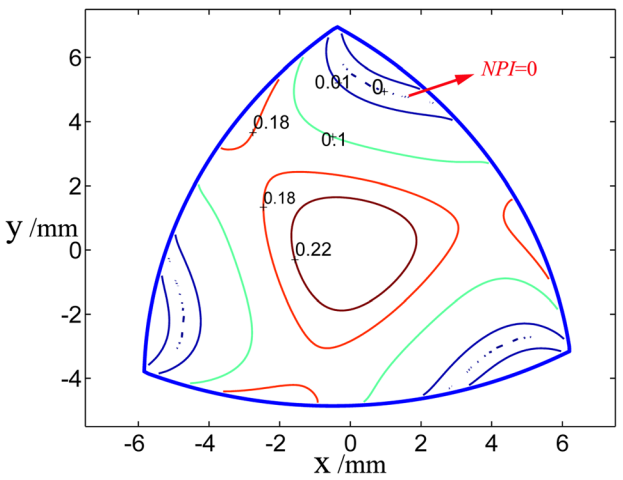

Fig. 8 Distribution of the index in the translational workspace with rotational angle $\varphi = -30$ deg

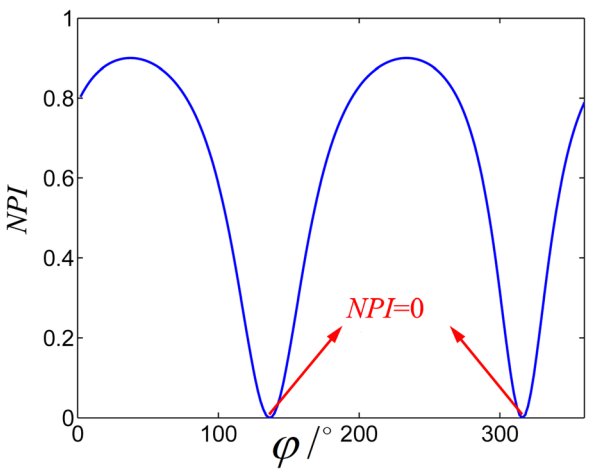

Fig. 9 Relationship between index and rotational angles with constant position: $x = 0, y = 0$

From Figs. 8 and 9, one can see certain points with index equaling to zero, NPI = 0, indicating that the transmission force cannot transmit any force/torque out in these configurations. Actually, the zero-value points are regarded to the parallel singular

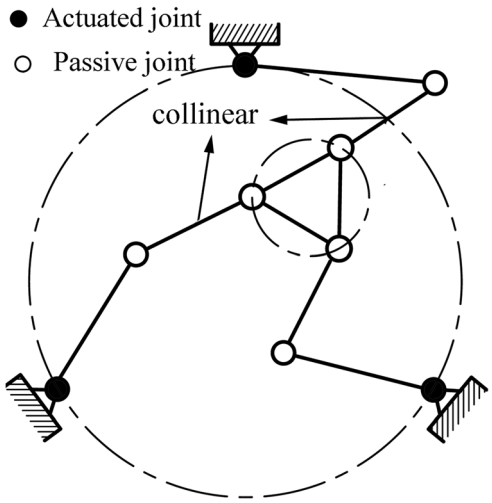

Fig. 10 A parallel singular configuration when the moving platform locates at $x = 1, y = 5.2$ and $\varphi = -30$ deg

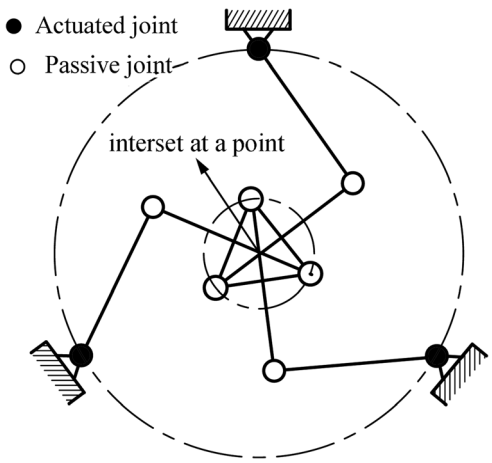

Fig. 11 A parallel singular configuration when the moving platform locates at $x = 0, y = 0$ and $\varphi = 136$ deg

configurations [18] shown in Figs. 10 and 11, respectively. Figure 10 shows a singular configuration with coordinates $x = 1, y = 5.2$ and $\varphi = -30$ deg, where two of the limbs are collinear. As shown in Fig. 11, three passive limbs intersect at a point, yielding a parallel singularity, when the manipulator locates at the configuration: $x = 0, y = 0$ and $\varphi = 136$ deg. For both cases, any torque load around the common intersection of the wrench screws needs infinite magnitudes of internal transmission forces to resist.

3.3 Six-Dimensional Spatial Parallel Manipulators

Example 3: 3-RPS Parallel Manipulator. Besides some typical planar parallel manipulators, other two spatial ones are taken as examples to illustrate the usage of the proposed index for the six-dimensional case. Figure 12 shows a prototype of 3-RPS parallel manipulator, which contains a moving platform, a base, and three identical RPS limbs connecting to the base and moving platform. The prismatic joints are actuated. This manipulator, being as a tool head, is widely used in machining application [19].

From force/torque analysis of this spatial parallel manipulator, the mobile platform is constrained by six TWSs which are all determined by the output wrench of the system. Each leg provides two TWSs, i.e., both pure forces passing through S joint, one of which, $\boldsymbol{e}_{i1}$, is collinear with the axis of the limb, and the other one, $\boldsymbol{e}_{i2}$, is parallel to the axis of the R joint (Fig. 12). All the pitches of

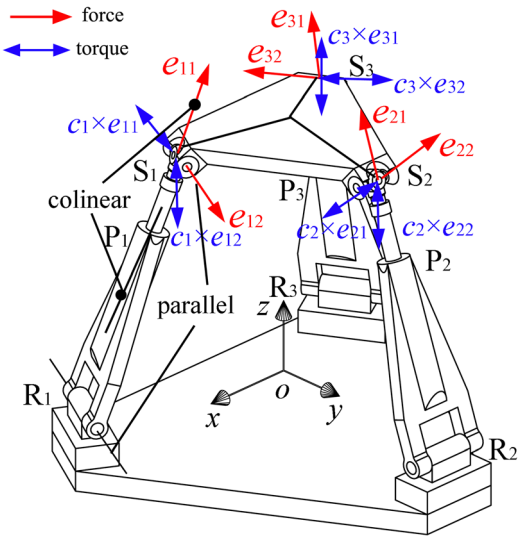

Fig. 12 A spatial 3-RPS parallel manipulator

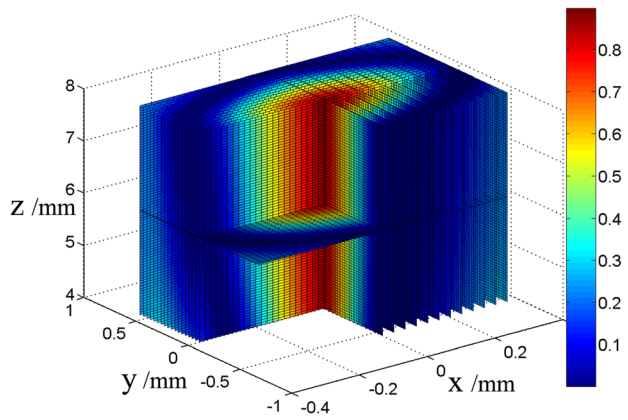

Fig. 13 Distribution atlas of the index in the chosen spatial workspace

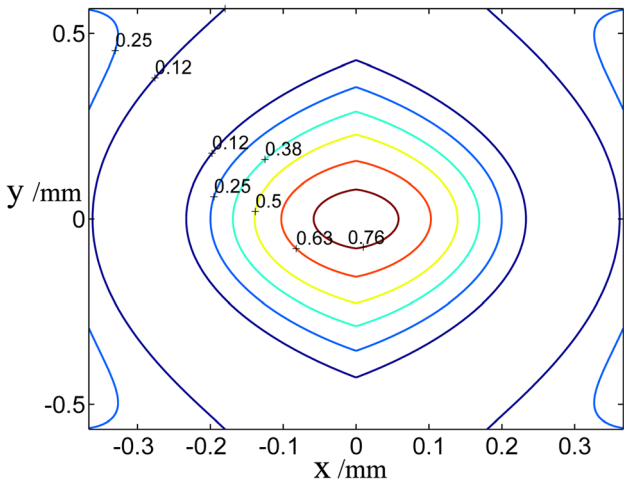

Fig. 14 Distribution atlas of the index in the selected slice with change of x- and y-coordinates when fixing z-axis, $z = 6$

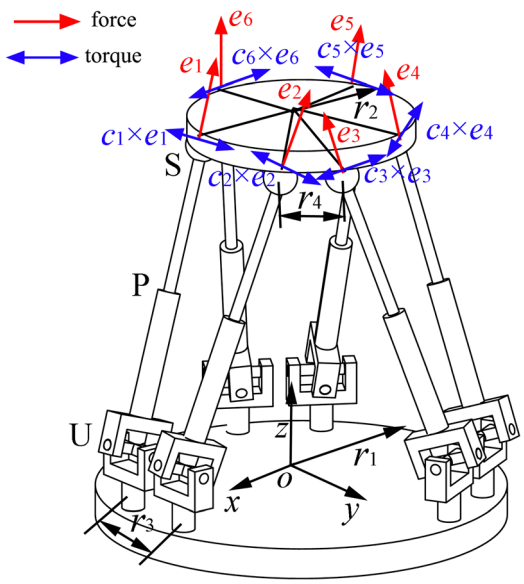

Fig. 15 A spatial Stewart manipulator

the six pure forces are zero, and the vectors pointing at the action point of TWSs ($S_i (i = 1, 2, 3)$) from the center of the platform are denoted as $\boldsymbol{c}_i (i = 1, 2, 3)$. Based on Eq. (5), we can achieve the transmission matrix as

$$\boldsymbol{E} = \begin{bmatrix} \boldsymbol{e}_{11}^{\mathrm{T}} & \boldsymbol{e}_{12}^{\mathrm{T}} & \cdots & \boldsymbol{e}_{31}^{\mathrm{T}} & \boldsymbol{e}_{32}^{\mathrm{T}} \\ (\boldsymbol{c}_1 \times \boldsymbol{e}_{11})^{\mathrm{T}} & (\boldsymbol{c}_1 \times \boldsymbol{e}_{12})^{\mathrm{T}} & & (\boldsymbol{c}_3 \times \boldsymbol{e}_{31})^{\mathrm{T}} & (\boldsymbol{c}_3 \times \boldsymbol{e}_{32})^{\mathrm{T}} \end{bmatrix} \tag{26}$$

Then, from Eq. (22), we can yield the index, as a six-dimensional case, for the 3-RPS parallel manipulator

$$\mathrm{NPI} = \frac{3}{(1/\sigma_1^2 + 1/\sigma_2^2 + \ldots + 1/\sigma_6^2)} \tag{27}$$

With respect to the global coordinate system: o-xyz coordinate is attached to the base, the position of the moving platform can be indicated as (x, y, z), and the orientations can be described by tilt-and-torsion angles (ϕ, θ, φ) [20]. As analyzed in Ref. [19], the manipulator retains three DOFs (two rotational and one translational DOF) while performing another two translational DOFs, termed parasitic motions. For the sake of convenience, we use three translational components (x, y, z) to represent the task space. Without loss of generality, we assume the geometric parameters of the manipulator: the radius of the moving platform, $\|\boldsymbol{c}_i\| = 1 (i = 1, 2, 3)$, and the radius of the base, $oR_i = 1.5$ $(i = 1, 2, 3)$.

Figure 13 shows the distribution atlas of the NPI index in the chosen spatial workspace: $x \in [-0.4, 0.4]$, $y \in [-0.6, 0.6]$, and $z \in [4, 8]$. Figure 14 manifests the distribution of the index in the selected middle slice with change of x- and y-axes when fixing z-axis as $z = 6$. The results indicate that the index indeed ranges from zero to unity. The manipulator performs better force/torque transmission performance when the mobile platform stays closer to the original point, $(x, y) = (0, 0)$. Also we can find that the index get larger when the extensible limbs extend further, i.e., value of z-axis gets larger.

Example 4: Stewart Parallel Manipulator. The architecture behind the famous Stewart mechanism [21] is a spatial 6-UPS kinematic mechanism (Fig. 15). Its moving platform connects the base through six identical UPS limbs, each of which includes a U joint, an actuated P joint, and S joint in series. Without loss of generality, we set the parameters, the radius of the moving platform, $r_2 = 1$, the radius of the base, $r_1 = 2$, and the offsetting lengths, $r_3 = r_4 = 0.35$. The position of the moving platform can

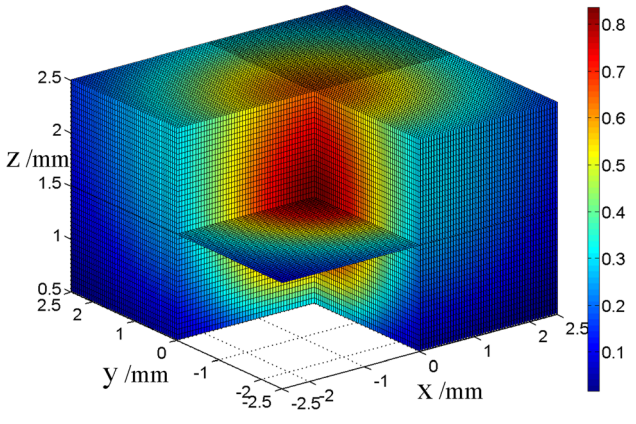

Fig. 16 Distribution of the index in the translational spatial workspace while fixing the three rotational angles as zero

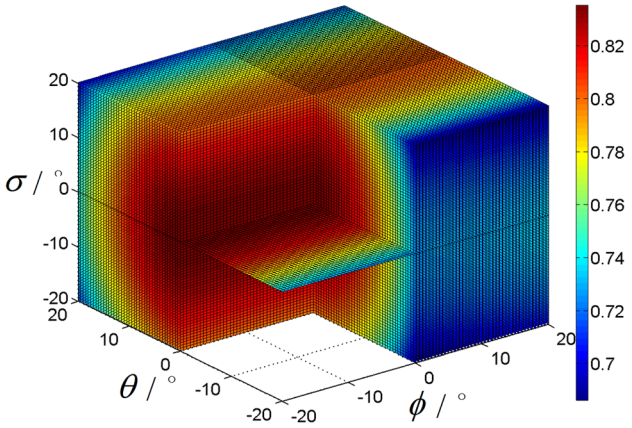

Fig. 18 Distributions of the index in a rotational workspace while fixing translational coordinates as $x, y = 0$, and $z = 1.5$

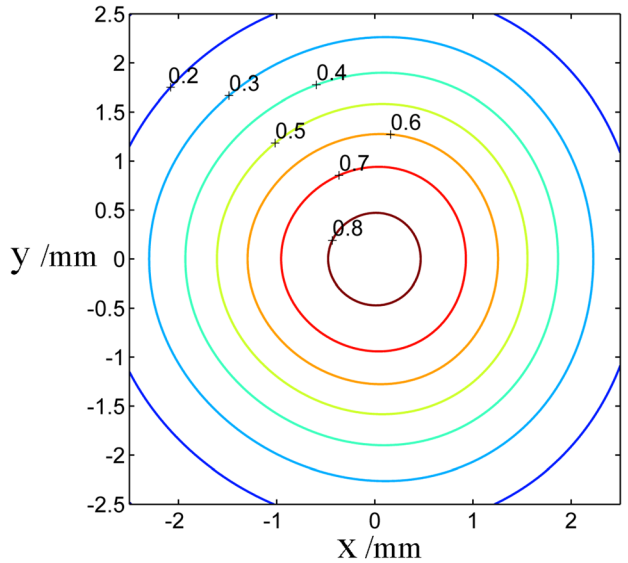

Fig. 17 Distribution of the index in the selected middle slice by fixing the *z*-axis and three rotational angles, $z = 1.5$, $\phi = 0, \theta = 0, \varphi = 0$

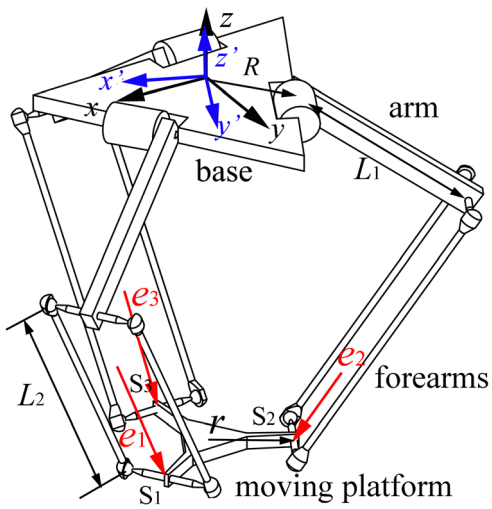

Fig. 19 A spatial Delta robot

be described by (x, y, z), while the tilt-and-torsion angles (ϕ, θ, φ) are used to describe the orientation of the platform.

Each UPS limb provides a TWS, a pure force, passing through S joint along the direction of the limb. Then from Eq. (22), we can achieve the index for the Stewart manipulator as

$$\text{NPI} = \frac{3}{(1/\sigma_1^2 + 1/\sigma_2^2 + \ldots + 1/\sigma_6^2)} \tag{28}$$

Here, we present the distribution of the NPI index in a spatial translational workspace while fixing three rotational angles as zero (Fig. 16). In order to show the details about the distribution values, Fig. 17 shows the contour distribution in one selected slice with the change of x–y coordinates by fixing the z-axis and three rotational angles as $z = 1.5$, $\phi = 0$, $\theta = 0$, and $\varphi = 0$, respectively. Figure 18 presents the distribution in a rotational workspace of this manipulator while fixing the translational coordinates as $x, y = 0$ and $z = 1.5$.

4 Comparison Analysis Between Different Indices

As mentioned, performance evaluation is one of the most significant issues in analyzing and designing parallel robots. Several approaches and indices were introduced to evaluate the performance of parallel manipulators in different aspects. Such as the well-known local conditioning index (LCI) derived from the Jacobian matrix was used to measure the mapping between inputs and output [22]. LCI index was widely accepted and applied in performance analysis in both serial and parallel mechanisms [23]. However, certain recent research noticed that it encounters some limitations in the analysis of parallel manipulators, which could be drawn at least as follows [12,24]:

(1) Unit inhomogeneous problem when it is applied in the mixed-DOF parallel manipulator causing by inconsistence of units, i.e., the units of translational DOF and rotational DOF are different.
(2) Coordinates dependent property due to that the Jacobian matrix is dependent to the coordinates.

Many researchers attempted to address the above problems, such as introducing the concept of characteristic/natural length [25]. However, the LCI values would accordingly vary with the change of frame coordinates. It is not an intuitive way for different end users, because they would achieve different results to the same parallel manipulator from different coordinates. Conversely, the proposed NPI index measures the mapping between the output forces/torques and the constraint forces, similar to the concept of transmission angle or pressure angle. Based on screw theory, the index could be used to analyze all exact-constraint parallel

manipulators including mixed-DOF ones. Besides, the index is a frame-independent one which could be demonstrated from an example as follows.

Example 5: Delta Robot. Here, we select a typical Delta robot as an example to give comparison study between proposed NPI index and existing index LCI. The Delta robot (Fig. 19) is considered to be one of the fastest parallel robots nowadays [26]. The mechanism contains a base, a moving platform, and three identical kinematic limbs including arms and forearms (parallel pantograph structure). This manipulator is regarded as a pure translational mechanism, which generates three translational DOFs. We assume the parameters of Delta robot freely for comparison analysis: the radii of base and moving platform are $r = 1$, $R = 2$, respectively, and the lengths of arm and forearm are $L_1 = 3$ and $L_2 = 5$, respectively. For comparison study, we set two coordinates, i.e., o-xyz and o-$x'y'z'$, in the base platform shown in Fig. 19.

According to Eq. (22), we can define the NPI index of Delta robot as

$$\mathrm{NPI} = \frac{3}{(1/\sigma_1^2 + 1/\sigma_2^2 + 1/\sigma_3^2)} \tag{29}$$

where $\sigma_i (i = 1, 2, 3)$ is the singular value of transmission matrix $\boldsymbol{E}$.

It is well-known that there is no rotational outputs in the Delta robot, thereby, the torques acting on the platform do not create any work. Hence, the genuine TWSs of this manipulator are only three pure forces, $\boldsymbol{e}_i (i = 1, 2, 3)$. Here, we can achieve the equivalent transmission matrix as

$$\boldsymbol{E} = \begin{bmatrix} \boldsymbol{e}_1^{\mathrm{T}} & \boldsymbol{e}_2^{\mathrm{T}} & \boldsymbol{e}_3^{\mathrm{T}} \end{bmatrix} \tag{30}$$

Based on the method proposed in Ref. [21], we could calculate the LCI of Delta robot. Figure 20(*a*) shows the distribution of the LCI index in the chosen workspace with respect to o-xyz coordinate, while Fig. 20(*b*) presents the distribution of the LCI index in the same workspace but with respect to o-$x'y'z'$ coordinate. From Figs. 20(*a*) and 20(*b*), one can see that the LCI index varies with the change of coordinates. That is to demonstrate that the existing LCI index is frame-dependent. On the other hand, Figs. 21(*a*) and 21(*b*) illustrate the distribution atlases of the proposed NPI index with respect to two coordinates o-xyz and o-$x'y'z'$, respectively. From the results, we could claim that the proposed NPI index keeps constant with different coordinates, that is, the NPI index is frame-independent.

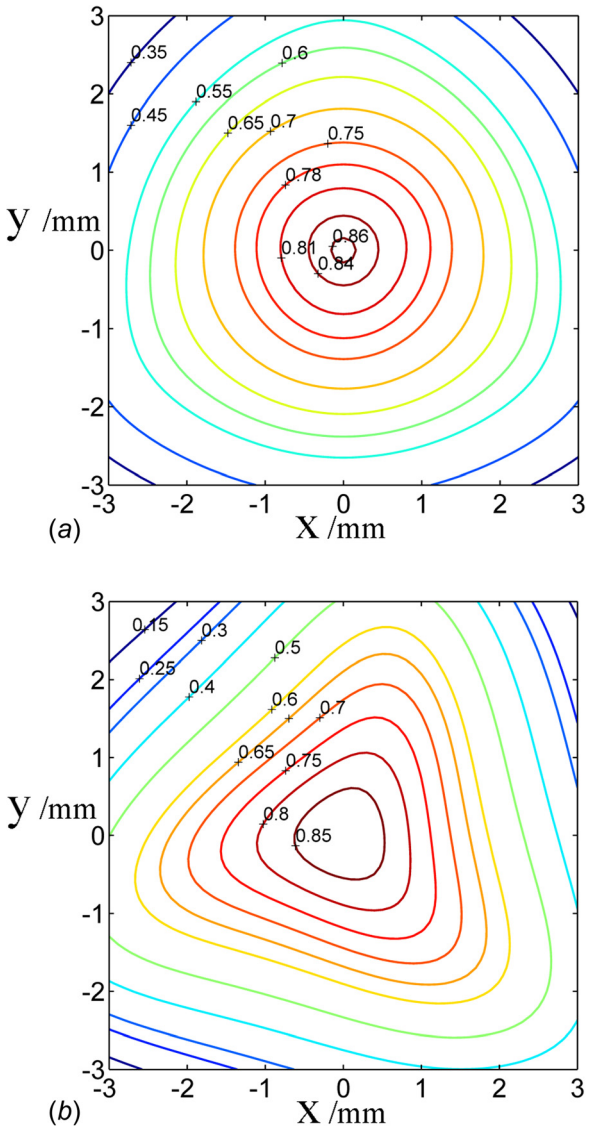

Fig. 20 Distribution of LCI index in the chosen workspace of Delta robot with respect to (*a*) *o-xyz* and (*b*) *o-x′y′z′* coordinates

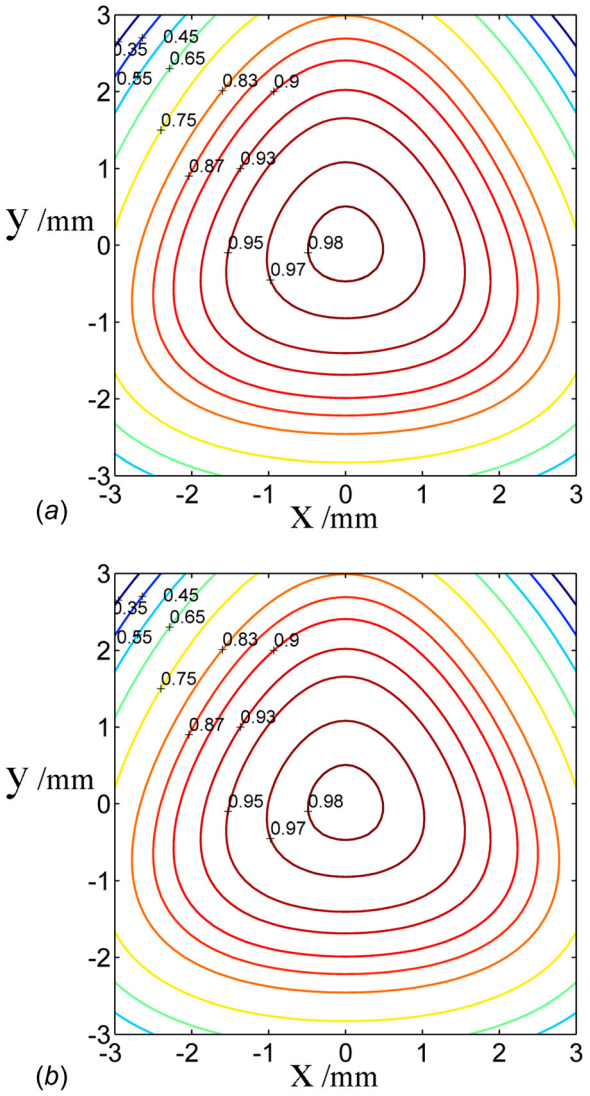

Fig. 21 Distribution of NPI index in the chosen workspace of Delta robot with respect to (*a*) *o-xyz*, and (*b*) *o-x′y′z′* coordinates

Besides, from comparison between Figs. 20 and 21, one can see that the overall tendency is similar, i.e., the Delta robot behaves better performances near the central points.

5 Conclusion

The internal forces and torques in a parallel mechanism contribute to manipulating the end-effector and resisting the external loads. The force/torque transmission quality reflects the essential performance of a parallel manipulator. A generalized force/torque transmission index, the NPI, is proposed here for multiDOF parallel manipulators. This index is rooted on the concepts of pressure angle or transmission angle in single DOF one. Since the transmission matrix is spanned by the TWSs, this index measures the total magnitude of the transmission wrenches. The unit load wrench is applied and the unit characteristic length is scaled for a uniform performance evaluation and comparison. The index is normalized against its lower bound, thus it ranges from zero to unity. Furthermore, several parallel manipulators including the two-, three-, and six-dimensional cases are taken as examples to illustrate the usage of the proposed approach and index. The performance atlas shows the force/torque transmission distribution of the parallel manipulators. The worst scenario indicated by this proposed index happens when the magnitude of the transmission wrenches reaches infinity, caused by parallel singularity.

By comparing different indices, the NPI index stands out with the merits of unit-homogenous and frame-independency. The index considers the translational and rotational DOFs together aiming at resolving all the exactly constrained parallel manipulators including the mixed-DOF ones. Moreover, the proposed NPI index could be used together with other indices as criteria in different aspects in optimal designs of parallel manipulators. The optimization based on this index will be investigated in our further researches.

Acknowledgment

This project was supported by National Natural Science Foundation of China (NSFC) (Grant Nos. 51375251, 51425501, and 51135008).

References

[1] Patel, Y. D., and George, P. M., 2012, "Parallel Manipulators Applications—A Survey," Mod. Mech. Eng., **2**(3), pp. 57–64.
[2] Togai, M., 1986, "An Application of the Singular Value Decomposition to Manipulability and Sensitivity of Industrial Robots," SIAM J. Algebraic Discrete Meth., **7**(2), pp. 315–320.
[3] Dubey, R., and Luh, J. Y. S., 1988, "Redundant Robot Control Using Task Based Performance Measures," J. Rob. Syst., **5**(5), pp. 409–432.
[4] Firmani, F., Zibil, A., Nokleby, S. B., and Podhorodeski, R. P., 2008, "Wrench Capabilities of Planar Parallel Manipulators. Part I: Wrench Polytopes and Performance Indices," Robotica, **26**(6), pp. 791–802.
[5] Kim, S. G., and Ryu, J., 2003, "New Dimensionally Homogeneous Jacobian Matrix Formulation by Three End-Effector Points for Optimal Design of Parallel Manipulators," IEEE Trans. Rob. Autom., **19**(4), pp. 731–737.
[6] Salisbury, J. K., and Craig, J. J., 1982, "Articulated Hands: Force Control and Kinematic Issues," Int. J. Rob. Res., **1**(1), pp. 4–17.
[7] Yoshikawa, T., 1985, "Manipulability of Robotic Mechanisms," Int. J. Rob. Res., **4**(2), pp. 3–9.
[8] Duffy, J., 1996, *Statics and Kinematics With Applications to Robotics*, Cambridge University Press, New York.
[9] Prajapati, J. M., and Patel, L. N., 2007, "Dynamic (Forward and Inverse Force Transmission Capability) Analysis of the Stewart Platform as Robot Manipulator," IEEE International Conference on Mechatronics and Automation (ICMA 2007), Harbin, China, Aug. 5–8, pp. 2848–2853.
[10] Merlet, J. P., 1998, "Efficient Estimation of the Extremal Articular Forces of a Parallel Manipulator in a Translation Workspace," IEEE International Conference on Robotics and Automation, Leuven, Belgium, May 16–20, pp. 1982–1987.
[11] Kim, H. S., and Choi, Y. J., 2001, "Forward/inverse Force Transmission Capability Analyses of Fully Parallel Manipulators," IEEE Trans. Rob. Autom., **17**(4), pp. 526–531.
[12] Merlet, J. P., 2006, "Jacobian, Manipulability, Condition Number, and Accuracy of Parallel Robots," ASME J. Mech. Des., **128**(1), pp. 199–206.
[13] Kosuge, K., Okuda, M., Kawamata, H., and Fukuda, T., 1993, "Input/Output Force Analysis of Parallel Link Manipulators," IEEE International Conference on Robotics and Automation, Atlanta, GA, May 2–6, pp. 714–719.
[14] Chen, C., and Angeles, J., 2007, "Generalized Transmission Index and Transmission Quality for Spatial Linkages," Mech. Mach. Theory, **42**(9), pp. 1225–1237.
[15] Tsai, M. J., and Lee, H. W., 1994, "The Transmissivity and Manipulability of Spatial Mechanisms," ASME J. Mech. Des., **116**(1), pp. 137–143.
[16] Hunt, K. H., 1990, "Kinematic Geometry of Mechanisms," Oxford University Press, New York.
[17] Angeles, J., 2006, *Fundamentals of Robotic Mechanical Systems: Theory, Methods, and Algorithms*, 3rd ed., Springer-Verlag, New York.
[18] Bonev, I. A., Zlatanov, D., and Gosselin, C. M., 2003, "Singularity Analysis of 3-DOF Planar Parallel Mechanisms Via Screw Theory," ASME J. Mech. Des., **125**(3), pp. 573–581.
[19] Chen, X., Xie, F. G., Liu, X-J, Xie, F., and Sun, T., 2014, "A Comparison Study on Motion/Force Transmissibility of Two Typical 3-DOF Parallel Manipulators: The Sprint Z3 and A3 Tool Heads," Int. J. Adv. Rob. Syst., **11**(5), pp. 1–10.
[20] Liu, X.-J., and Bonev, I. A., 2008, "Orientation Capability, Error Analysis, and Dimensional Optimization of Two Articulated Tool Heads With Parallel Kinematics," ASME J. Manuf. Sci. Eng., **130**(1), p. 011015
[21] Dasgupta, B., and Mruthyunjaya, T. S., 2000, "The Stewart Platform Manipulator: A Review," Mech. Mach. Theory, **35**(1), pp. 15–40.
[22] Gosselin, C., and Angeles, J., 1989, "The Optimum Kinematic Design of a Spherical Three-Degree-of-Freedom Parallel Manipulator," ASME J. Mech. Des., **111**(2), pp. 202–207.
[23] Liu, X-J., Wang, J. S., and Kim, J. W., 2006, "Determination of the Link Lengths for a Spatial 3-DOF Parallel Manipulator," ASME J. Mech. Des., **128**(2), pp. 365–373.
[24] Wang, J. S., Wu, C., and Liu, X-J., 2010, "Performance Evaluation of Parallel Manipulators: Motion/Force Transmissibility and Its Index," Mech. Mach. Theory, **45**(10), pp. 1462–1476.
[25] Angeles, J., 2006, "Is There a Characteristic Length of a Rigid-Body Displacement?," Mech. Mach. Theory, **41**(8), pp. 884–896.
[26] Pierrot, F., Reynaud, C., and Fournier, A., 1990, "Delta: A Simple and Efficient Parallel Robot," Robotica, **8**(2), pp. 105–109.